



1



2



3

Fourier-enhanced Implicit Neural Fusion Network for Multispectral and Hyperspectral Image Fusion

Yu-Jie Liang ^{#1}

yujieliang0219@gmail.com

Zihan Cao ^{#1}

iamzihan666@gmail.com

Shangqi Deng ²

shangqideng0124@gmail.com

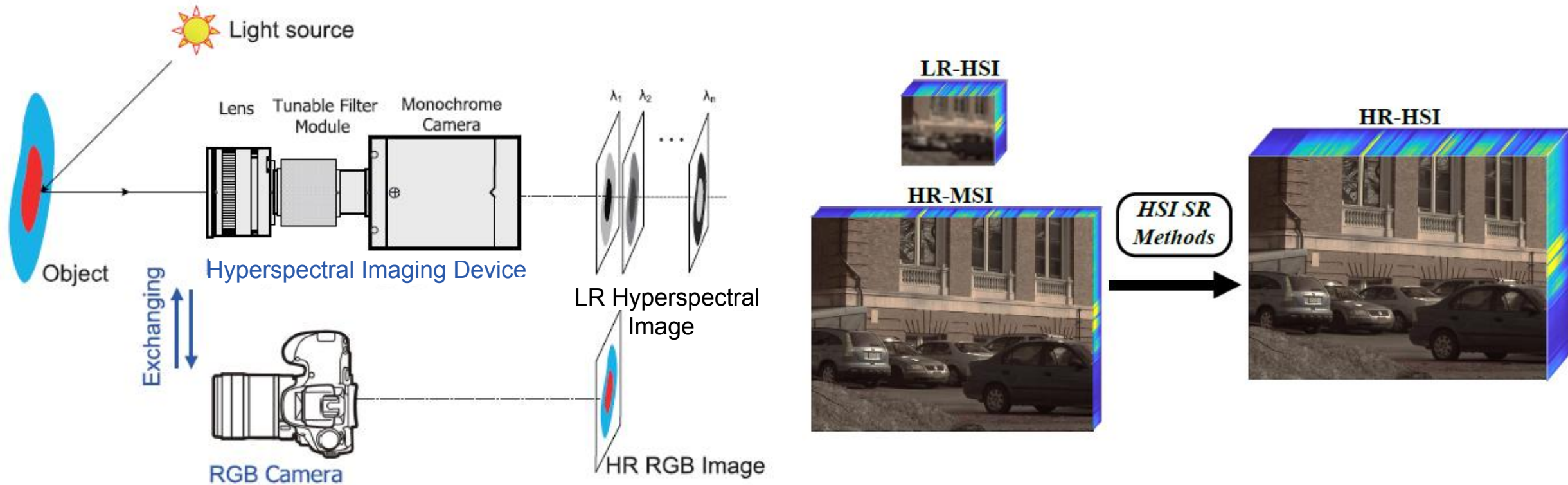
Hong-Xia Dou ³

hongxiadou1991@126.com

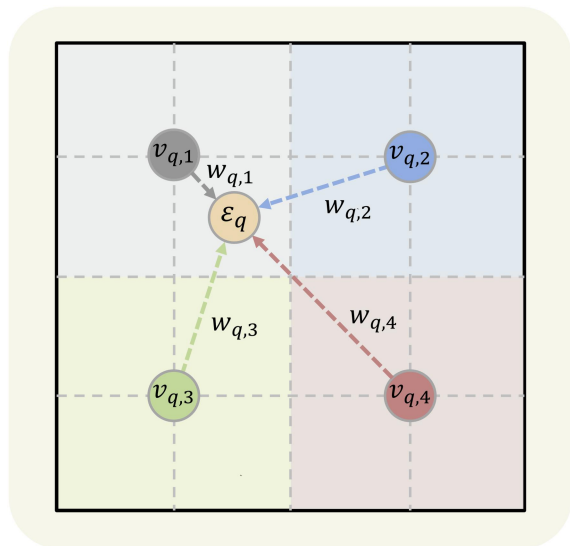
Liang-Jian Deng ^{*1}

liangjian.deng@uestc.edu.cn

Multispectral and Hyperspectral Image Fusion



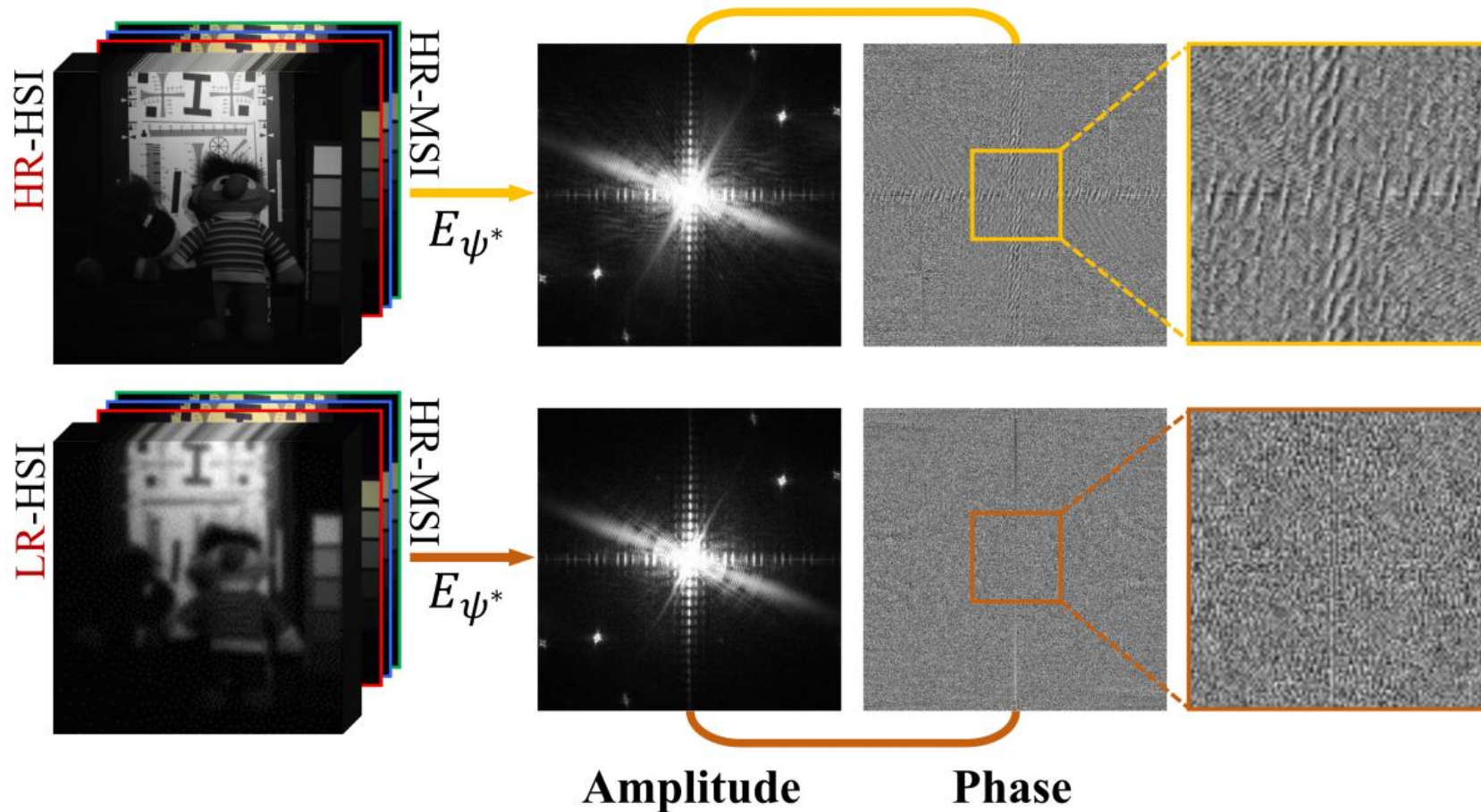
Preliminary and Motivation



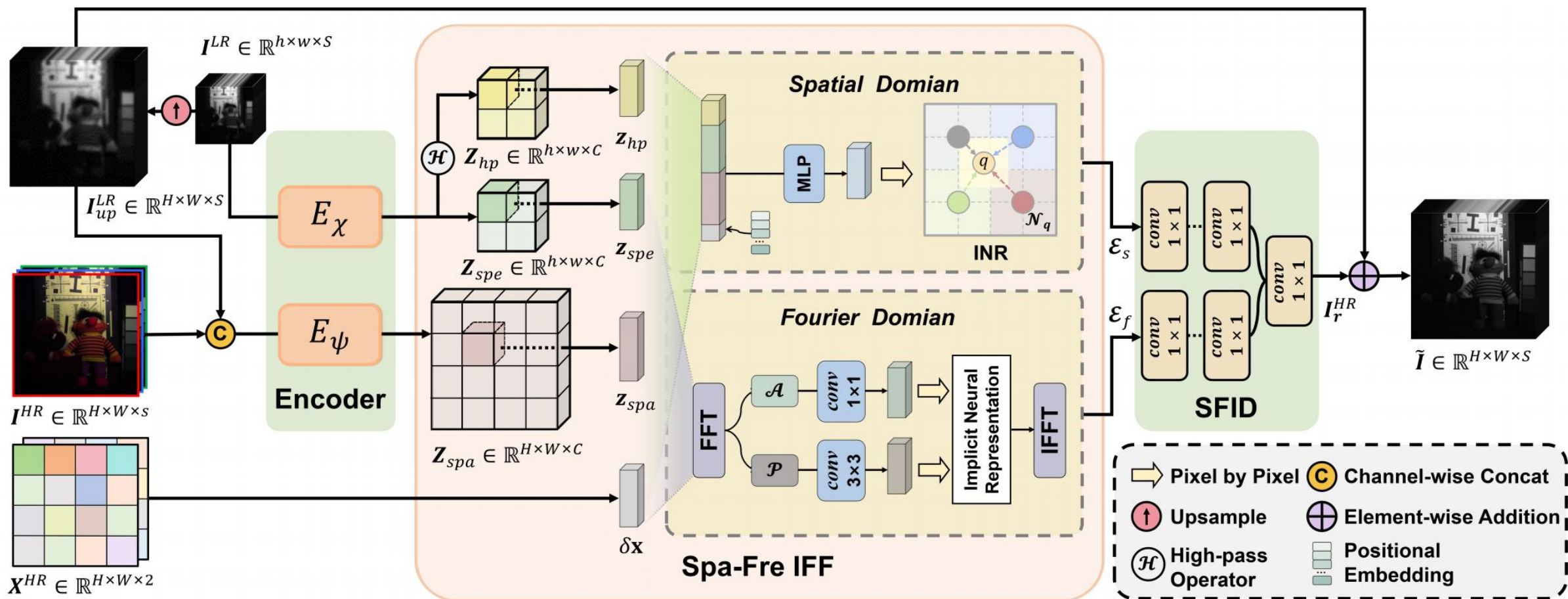
$$\hat{\mathbf{I}}(\mathbf{x}_q) = \sum_{i \in \mathcal{N}_q} w_{q,i} \mathbf{v}_{q,i}$$

$$w_{q,i} = S_i / S$$

$$\mathbf{v}_{q,i} = \phi_{\theta}(\mathbf{z}_i, \mathbf{x}_q - \mathbf{x}_i)$$



FeINFN Framework



Spatial-Frequency Implicit Fusion Function

- **INR Encoder Networks**

The INR encoders try to extract spatial and spectral latent codes:

$$\mathbf{Z}_{spe} = E_{\chi}(\mathbf{I}^{LR}), \quad \mathbf{Z}_{spa} = E_{\psi}(\text{Cat}(\mathbf{I}_{up}^{LR}, \mathbf{I}^{HR}))$$

- **Spatial-Frequency Implicit Fusion Function**

Spatical Domain:

$$\mathbf{w}_{q,i}, \mathbf{v}_{q,i} = \phi_{\theta}(\mathbf{z}_{spe}, \mathbf{z}_{spa}, \mathbf{z}_{hp}, \gamma(\delta \mathbf{x}))$$

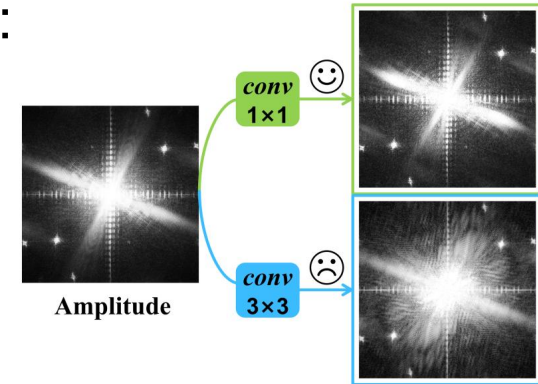
$$\boldsymbol{\varepsilon}_s = \sum_{i \in \mathcal{N}_q} \bar{\mathbf{w}}_{q,i} * \mathbf{v}_{q,i}$$

$\mathbf{z}_{hp} = \mathcal{H}(\mathbf{z}_{spe})$
 $\delta \mathbf{x} = \{\mathbf{x}_q - \mathbf{x}_{q,i}\}_{i \in \mathcal{N}_q}$
 $\gamma(\delta \mathbf{x}) = [\sin(2^0 \delta \mathbf{x}), \cos(2^0 \delta \mathbf{x}), \dots, \sin(2^{L-1} \delta \mathbf{x}), \cos(2^{L-1} \delta \mathbf{x})]$

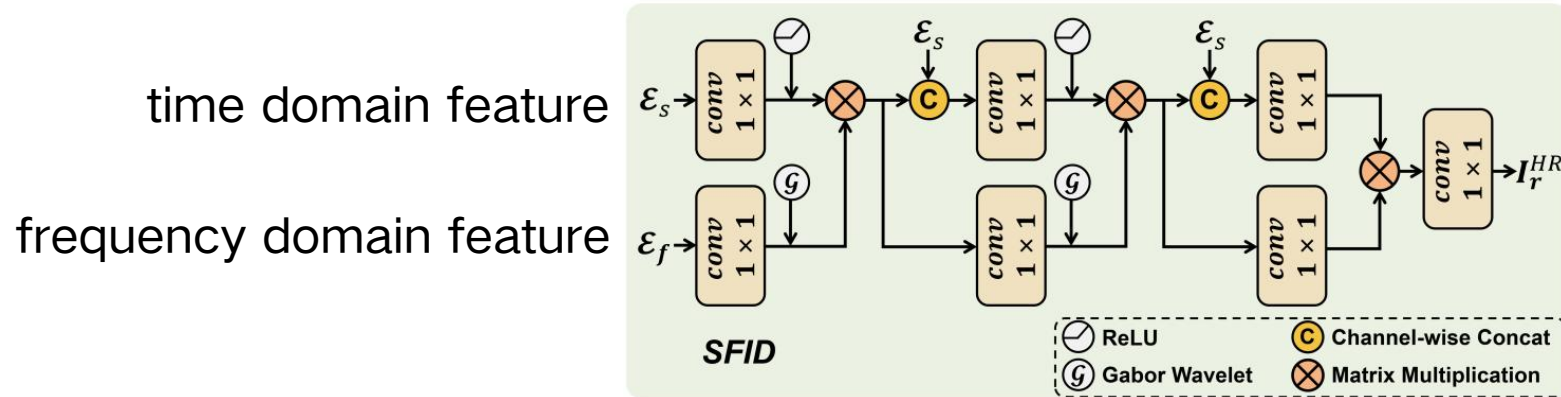
Frequency Domain: We employ FFT to transform latent codes from the spatial domain to the frequency domain, handling amplitude and phase separately:

$$\mathbf{w}_{q,i}^{\mathcal{A}}, \mathbf{v}_{q,i}^{\mathcal{A}} = \phi_{\alpha}^{\mathcal{A}}(\mathcal{A}(\mathbf{f}_{spe}), \mathcal{A}(\mathbf{f}_{spa}), \delta \mathbf{x}) \quad \mathcal{A}'_f = \sum_{i \in \mathcal{N}_q} \bar{\mathbf{w}}_{q,i}^{\mathcal{A}} * \mathbf{v}_{q,i}^{\mathcal{A}}$$

$$\mathbf{w}_{q,i}^{\mathcal{P}}, \mathbf{v}_{q,i}^{\mathcal{P}} = \phi_{\beta}^{\mathcal{P}}(\mathcal{P}(\mathbf{f}_{spe}), \mathcal{P}(\mathbf{f}_{spa}), \delta \mathbf{x}) \quad \mathcal{P}'_f = \sum_{i \in \mathcal{N}_q} \bar{\mathbf{w}}_{q,i}^{\mathcal{P}} * \mathbf{v}_{q,i}^{\mathcal{P}}$$



Spatial-Frequency Interactive Decoder



Theorem 1. *The complex Gabor wavelet activation $\mathcal{G}(\mathbf{x}) = e^{j\omega_0\mathbf{x}} e^{-|v_0\mathbf{x}|^2}$ has the time-frequency tightness property. Moreover, from the perspective of signal spectrum analysis, this activation helps the decoder learn the optimal bandwidths.*

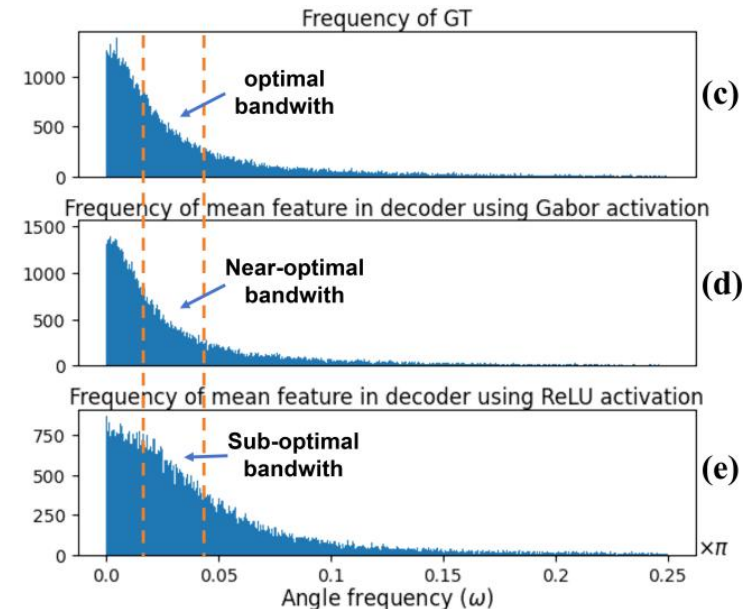
Time domain Tightness:

$|\mathcal{G}(\mathbf{x})|$ is primarily concentrated around $\mathbf{x}=0$ due to the exponential decay term.

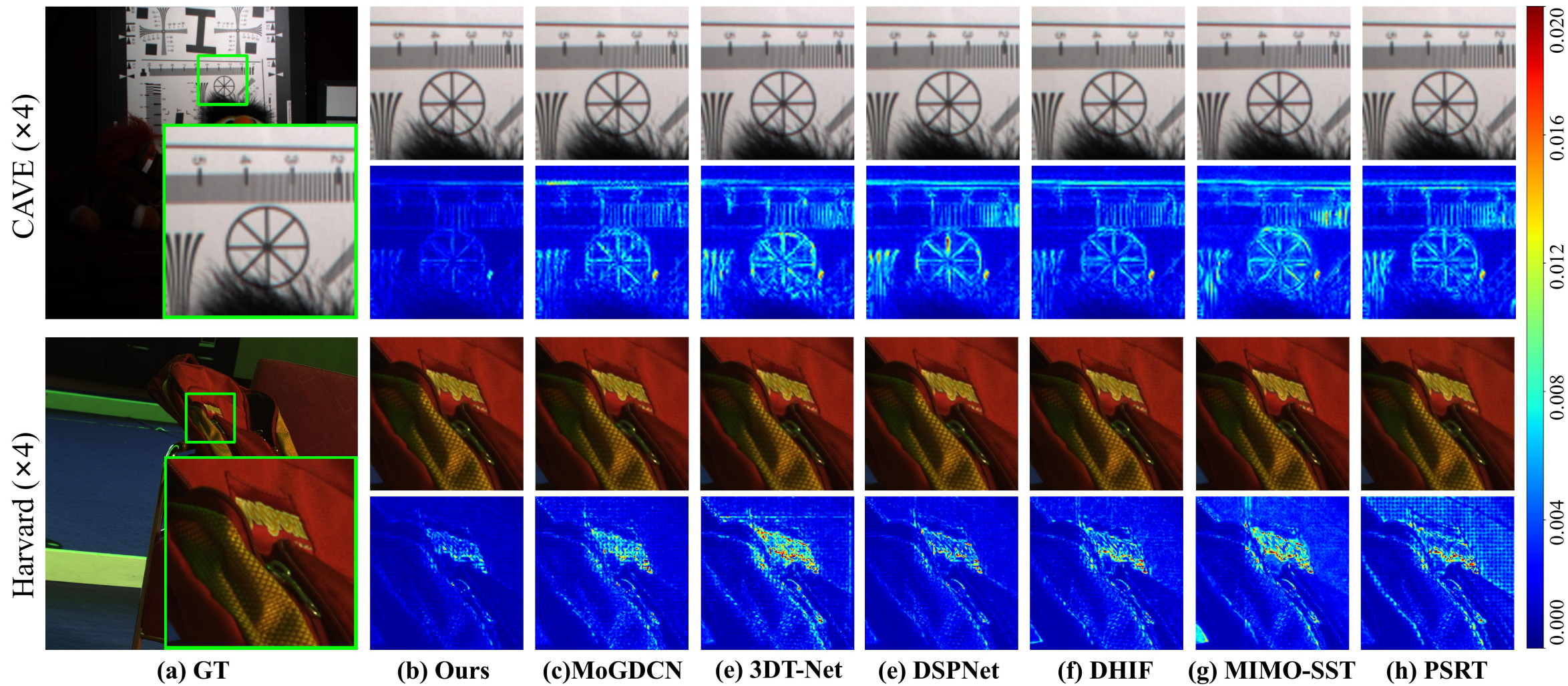
Frequency domain Tightness:

$$\mathcal{F}[\mathcal{G}(\mathbf{x})] = \int e^{j\omega_0\mathbf{x}} e^{-|v_0\mathbf{x}|^2} e^{-j\omega\mathbf{x}} d\mathbf{x}.$$

Uncertainty principle: $|\omega_0| \cdot v_0 \geq \frac{1}{4\pi}$



Experiments



Experiments

Methods	CAVE $\times 4$					Harvard $\times 4$				
	PSNR(\uparrow)	SAM(\downarrow)	ERGAS(\downarrow)	SSIM(\uparrow)	#params	PSNR(\uparrow)	SAM(\downarrow)	ERGAS(\downarrow)	SSIM(\uparrow)	#params
Bicubic	34.33 \pm 3.88	4.45 \pm 1.62	7.21 \pm 4.90	0.944 \pm 0.029	–	38.71 \pm 4.33	2.53 \pm 0.67	4.45 \pm 1.81	0.948 \pm 0.027	–
CSTF-FUS [22]	34.46 \pm 4.28	14.37 \pm 5.30	8.29 \pm 5.29	0.866 \pm 0.075	–	39.15 \pm 3.45	6.93 \pm 2.69	4.66 \pm 1.81	0.914 \pm 0.049	–
LTTR [9]	35.85 \pm 3.49	6.99 \pm 2.55	5.99 \pm 2.92	0.956 \pm 0.029	–	40.88 \pm 3.94	4.01 \pm 1.27	4.03 \pm 2.18	0.957 \pm 0.035	–
LTMR [8]	36.54 \pm 3.30	6.71 \pm 2.19	5.39 \pm 2.53	0.963 \pm 0.021	–	42.06 \pm 3.56	3.51 \pm 0.99	3.59 \pm 2.03	0.970 \pm 0.020	–
IR-TenSR [45]	35.61 \pm 3.45	12.30 \pm 4.68	5.90 \pm 3.05	0.945 \pm 0.027	–	40.47 \pm 3.04	4.36 \pm 1.52	5.57 \pm 1.57	0.963 \pm 0.014	–
ResTFNet [24]	45.58 \pm 5.47	2.82 \pm 0.70	2.36 \pm 2.59	0.993 \pm 0.006	2.387M	45.94 \pm 4.35	2.61 \pm 0.69	2.56 \pm 1.32	0.985 \pm 0.008	2.387M
SSRNet [52]	48.62 \pm 3.92	2.54 \pm 0.84	1.63 \pm 1.21	0.995 \pm 0.002	0.027M	48.00 \pm 3.36	2.31 \pm 0.60	2.30 \pm 1.42	0.987 \pm 0.007	0.027M
HSRNet [16]	50.38 \pm 3.38	2.23 \pm 0.66	1.20 \pm 0.75	0.996 \pm 0.001	0.633M	48.29 \pm 3.03	2.26 \pm 0.56	1.87 \pm 0.81	0.988 \pm 0.006	0.633M
MogDCN [10]	51.63 \pm 4.10	2.03 \pm 0.62	1.11 \pm 0.82	0.997 \pm 0.002	6.840M	47.89 \pm 4.09	2.11 \pm 0.52	1.89 \pm 0.82	0.988 \pm 0.007	6.840M
Fusformer [15]	49.98 \pm 8.10	2.20 \pm 0.85	2.50 \pm 5.21	0.994 \pm 0.011	0.504M	47.87 \pm 5.13	2.84 \pm 2.07	2.04 \pm 0.99	0.986 \pm 0.010	0.467M
DHIF [17]	51.07 \pm 4.17	2.01 \pm 0.63	1.22 \pm 0.97	0.997 \pm 0.002	22.462M	47.68 \pm 3.85	2.32 \pm 0.53	1.95 \pm 0.92	0.988 \pm 0.007	22.462M
PSRT [7]	50.47 \pm 6.19	2.19 \pm 0.64	2.06 \pm 3.71	0.996 \pm 0.003	0.247M	47.96 \pm 3.21	2.18 \pm 0.55	1.89 \pm 0.86	0.988 \pm 0.006	0.247M
3DT-Net [25]	51.38 \pm 4.18	2.16 \pm 0.70	1.14 \pm 1.00	0.996 \pm 0.003	3.464M	47.78 \pm 4.42	2.04\pm0.51	1.98 \pm 0.86	0.989\pm0.006	3.464M
DSPNet [35]	51.18 \pm 3.92	2.15 \pm 0.64	1.13 \pm 0.82	0.997 \pm 0.002	6.064M	48.29 \pm 3.16	2.30 \pm 0.55	1.93 \pm 0.93	0.988 \pm 0.006	6.064M
MIMO-SST [11]	50.98 \pm 3.39	2.23 \pm 0.70	1.18 \pm 0.73	0.997 \pm 0.002	4.983M	47.08 \pm 5.56	2.09 \pm 0.53	2.07 \pm 0.82	0.988 \pm 0.007	4.983M
FeINFN(Ours)	52.47\pm4.10	1.91\pm0.59	0.98\pm0.74	0.998\pm0.002	3.165M	49.06\pm3.15	2.10 \pm 0.53	1.78\pm0.75	0.989 \pm 0.007	3.165M

Experiments

Table 2: Quantitative comparisons with other up-sampling methods on the CAVE ($\times 4$) dataset.

Methods	PSNR(\uparrow)	SAM(\downarrow)	ERGAS(\downarrow)	SSIM(\uparrow)	#params
Bilinear	52.23 \pm 4.40	1.92 \pm 0.60	1.03 \pm 0.86	0.997 \pm 0.0021	3.119M
Bicubic	52.22 \pm 4.31	1.95 \pm 0.61	1.02 \pm 0.82	0.997 \pm 0.0021	3.119M
Pixel Shuffle	52.26 \pm 4.37	1.90\pm0.59	1.02 \pm 0.85	0.997 \pm 0.0022	3.057M
Our	52.47\pm4.10	1.91 \pm 0.59	0.98\pm0.74	0.998\pm0.0015	3.165M

Table 3: Quantitative comparisons with reduced models on the CAVE ($\times 4$) dataset. \mathcal{S} & \mathcal{F} mean the domain difference.

\mathcal{S}	\mathcal{F}	PSNR(\uparrow)	SAM(\downarrow)	ERGAS(\downarrow)	SSIM(\uparrow)	#params
✓	✗	52.11 \pm 4.22	1.95 \pm 0.59	1.04 \pm 0.82	0.998 \pm 0.0017	2.869M
✗	✓	47.86 \pm 3.42	3.49 \pm 1.30	1.67 \pm 1.13	0.995 \pm 0.0020	2.940M
✓	✓	52.47\pm4.10	1.91\pm0.59	0.98\pm0.74	0.998\pm0.0015	3.165M

Table 4: Quantitative comparisons with different activation functions in SFID on the CAVE ($\times 4$) dataset.

Nonlinear	PSNR(\uparrow)	SAM(\downarrow)	ERGAS(\downarrow)	SSIM(\uparrow)
ReLU	52.03 \pm 3.84	2.00 \pm 0.59	1.02 \pm 0.74	0.998\pm0.0013
GELU	51.96 \pm 3.88	2.01 \pm 0.60	1.03 \pm 0.75	0.998 \pm 0.0014
Leaky ReLU	51.98 \pm 3.92	2.01 \pm 0.60	1.03 \pm 0.76	0.998 \pm 0.0014
Our	52.47\pm4.10	1.91\pm0.59	0.98\pm0.74	0.998 \pm 0.0015

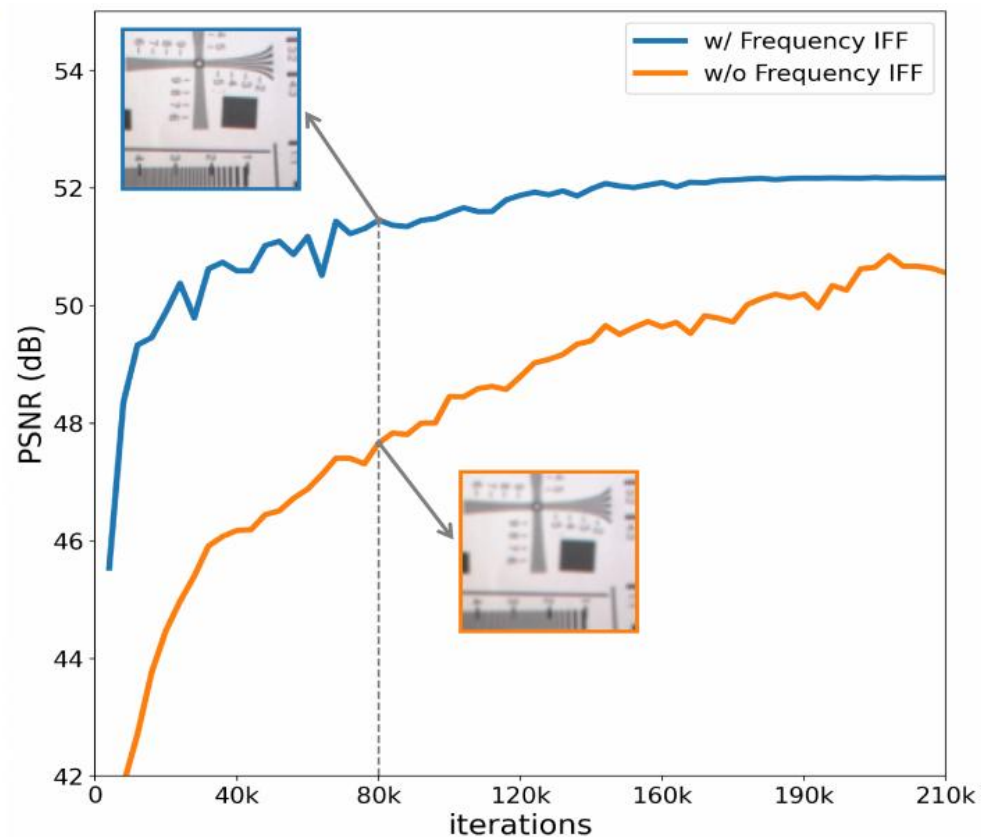
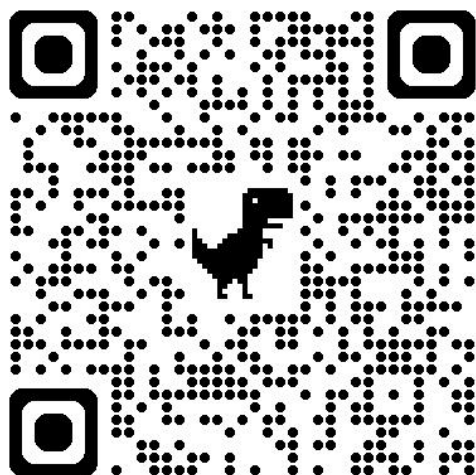


Figure 7: Changes in PSNR on the CAVE dataset of our FeINFN over iterations with and without the “Fourier Domain”. The Frequency IFF can help the network learn the high-frequency details and converge faster.

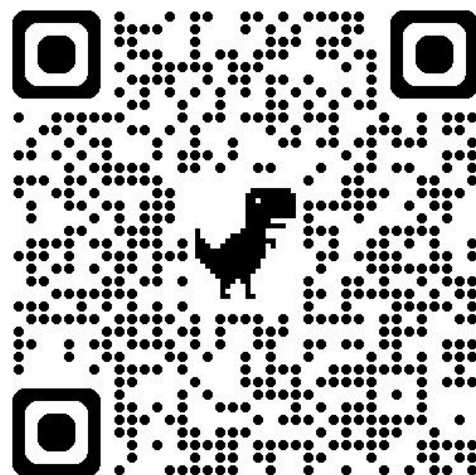


Thanks for your attention !

Paper



Code



Datasets

